Mechanics of Materials 41 (2009) 131–138

Contents lists available at ScienceDirect

Mechanics of Materials

journal homepage: www.elsevier.com/locate/mechmat

Resistance of grain boundary array to cleavage cracking in free-standing thin film

Jin Chen, Weiyi Lu, Yu Qiao *

Department of Structural Engineering, University of California – San Diego, La Jolla, CA 92093-0085, USA

ARTICLE INFO

Article history:
Received 15 January 2008
Received in revised form 12 October 2008

ABSTRACT

In a previous experimental study on free-standing silicon thin film, it was observed that cleavage front transmission across a through-thickness grain boundary could be considerably constrained by film surfaces. As a result, the boundary toughness was much lower than its bulk counterpart. In this study, inspired by the observation of crack front behaviors at triple grain boundary junctions, we perform a theoretical analysis on the fracture resistance of a regular grain boundary array in a thin film. The result indicates that as the cleavage front breaks down into a number of sections by the grain boundaries, the overall fracture resistance can be increased by nearly 60%. However, if the grain size is too small, the fracture resistance may decrease. The optimum grain size is around 1/5 to 1/4 of the film thickness. This finding provides a scientific basis for further experimental investigation on advanced processing techniques.

1. Introduction

Advanced technology for improving fracture resistance of thin solid films has been actively investigated for the past a few decades, promoted by the rapid development of semiconductor and micro/nano-fabrication industries (Madou, 2002). Many thin-film materials, such as silicon, silica, silicon carbides, etc., are intrinsically brittle. At working temperatures, very often they are at the lower-shelf of brittle-to-ductile transition region (Haque and Saif, 2003; Srikar and Spearing, 2003; Muhlstein, 2005; Boyce et al., 2007). When these materials are subjected to unexpected external loadings or internal stresses, catastrophic cracking can considerably limit their service lives (Bagdahn et al., 2003), especially in complex structures where a large number of micro-components interact with each other and failure of any of them may cause malfunction of the entire system. For instance, even with high-performance energy absorption housings made of reinforced polymers or shape-memory alloys, the drop resistance of electronics, e.g. cell phones and notebook computers, is still far from being satisfactory (Lau et al., 1998).

During processing and post-processing treatment of a brittle thin film, defects or irregular structural elements would be inevitably produced (Jackson, 2003). Once a short crack starts to grow, it can continue to propagate until the strain energy is consumed or the crack tip is arrested by obstacles. For semiconductor devices, usually due to the difficulties in manufacturing and the tight control of impurities, adding guest species as reinforcements is not an option. Thus, toughening them by optimizing their microstructures becomes an important way for preventing system failure.

In a homogeneous phase, cleavage cracking behavior is uniform. In order to increase local toughness, heterogeneous structures, such as grain boundaries, twin boundaries, and phase boundaries, must be created. Among these, grain boundaries usually offer the highest fracture resistance, which is one of the major reasons why most of microcracks are grain-sized (Hahn et al., 1959). Across a grain boundary, since the two grains are of different crystallographic orientations, a crack must change its surface from the cleavage plane of the first grain to that of the second one. A portion of grain boundary must be fractured or

* Corresponding author.
E-mail address: yqiao@ucsd.edu (Y. Qiao).

0167-6636/$ - see front matter © 2008 Elsevier Ltd. All rights reserved.
doi:10.1016/j.mechmat.2008.10.006

sheared apart geometrically necessarily; otherwise the separation of crack flanks cannot be completed. There are a number of factors that dominate the fracture resistance of a grain boundary. First, as the orientation of a crack varies, the net fracture surface area becomes different (Janssen, 2004). Second, the grain boundary area connecting crack surfaces across boundary demands additional work of separation (McClintock, 1997). Third, according to a recent experiment on large bicrystals (Qiao and Argon, 2003a,b), the break-through process of a cleavage front across a boundary is highly non-uniform. Most of the front would first be arrested by persistent grain boundary areas (PGBA), and the rest part would bow into the grain ahead of the boundary. Consequently, due to the shielding effect of the arrested front sections, the local crack growth driving force at the protruding part tends to decrease (Bakker, 1992; Wu, 2006), and thus a higher overall energy release rate is required (Qiao, 2005a,b). Finally, after the PGBAs fail, the cleavage front would break down into a number of sections that advance in parallel terrains, leading to the formation of river markings.

While for bulk materials grain boundary behaviors were analyzed extensively and the influences of grain size and crystallographic misorientations have been quite adequately understood (Gell and Smith, 1967; Kong and Qiao, 2005), their role in cleavage cracking in thin films is still relatively un-investigated, imposing tremendous challenges to grain boundary engineering study that is aimed at improving fracture resistance. Particularly, it is still unclear what would be the effects of grain size along the film thickness direction, or whether it is an important factor. In the following discussion, this problem will be analyzed in considerable detail.

2. Cleavage cracking in polycrystalline thin films

In order to understand the resistance of grain boundaries in thin films, we recently performed a microtensile experiment (Qiao and Chen, 2008), in which polycrystalline silicon was employed as a close analog to all the brittle semiconductors. Over the years, a large number of experiments and theoretical analyses have been carried out on fracture in silicon under various conditions (Kahn et al., 2001; Jensen et al., 2001; Beerschwinger et al., 1994, 1995; Sharpe et al., 1997; Greek et al., 1997, 1999; Schweitz and Ericson, 1999). In these work, usually the grain structure was not directly related to the fracture toughness, which could be an important reason for the large data scatters in testing results. In our experiment, the film thickness was 2–50 μm. In this thickness range, the grains were typically through-thickness, since those of unfavored orientations would be buried during film deposition process (Ohring, 1992). When the film thickness, t, was relatively large (40–50 μm), the cracking mode could be quite similar with that in a large bicrystal. As depicted in Fig. 1(a), as a cleavage front advanced from grain "A" to "B", it broke through the boundary in a few break-through windows (BTWs), which are indicated by "o" and "o*". With the increasing of external loading, the penetration depth increased. Eventually when the critical penetration depth was reached, the PGBA in between BTWs ("ocd" and "deo*") and the PGBAs near the film surface ("abo" and "fgo*") were separated apart, causing the unstable crack propagation. The crack front was broken down into a series of sections ("ac" and "ef"), advancing in parallel terrains shown by the shaded planes in grain "B". The borders of the terrains would be separated via shearing or secondary cleavage cracking, resulting in the formation of river mark-

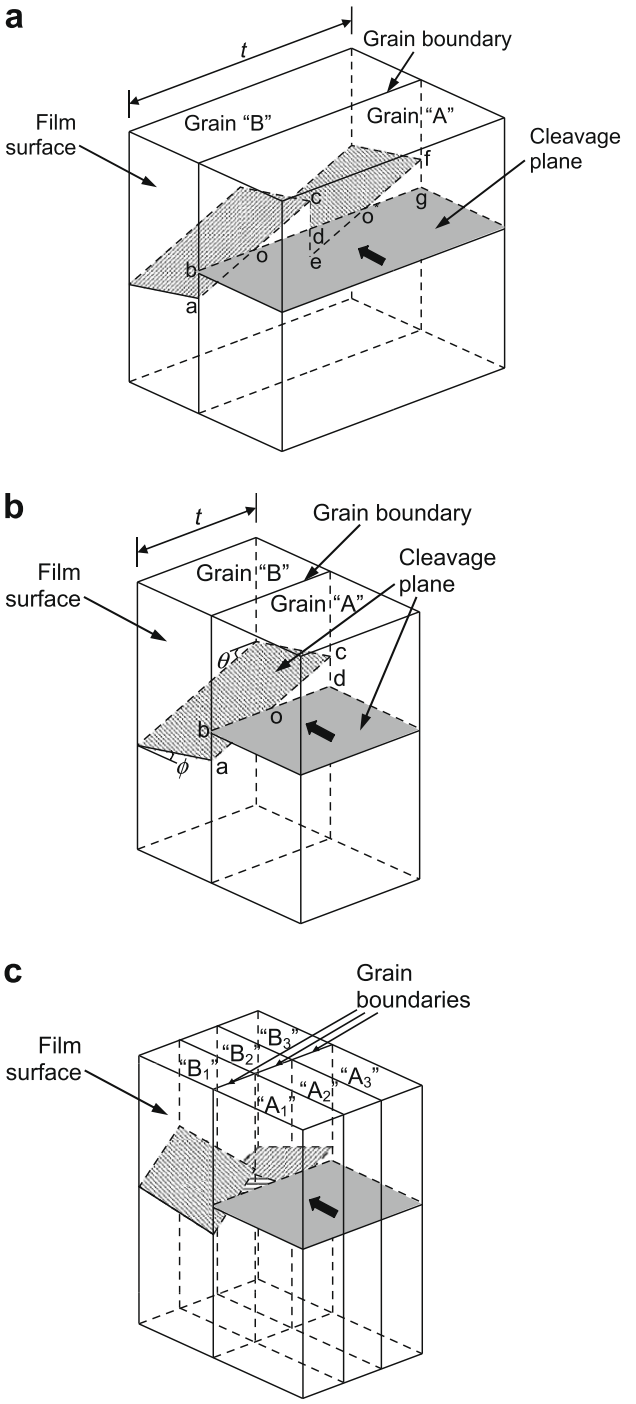

Fig. 1. Schematic diagrams of cleavage cracking (a) in a thick film of through-thickness grain boundary; and in thin films (b) of through-thickness grain boundary and (c) of multiple grain layers. The shaded areas indicate cleavage planes.

ings. The fracture resistance of the grain boundary was determined by the average behaviors of front sections, and thus was quite independent of the film thickness. When the film thickness was relatively small (2–10 μm), the film surfaces could significantly constrain the cleavage front transmission process across the boundary (Figs. 1b and 2). The space between the two free surfaces was sufficient for only one BTW. Under this condition, if the film thickness decreased, the resistance of PGBAs ("abo" and "cdo") would be reduced, and thus the boundary toughness, K_{cr}, was smaller. The experiment data show that as the film thickness changes from 10 μm to 2 μm, K_{cr} is lowered by 20–50%. That is, when the film thickness is comparable with BTW width, the fracture toughness is no longer a material constant, but decreases as t is lowered. This size effect is fundamentally different from the weakest link theory (Jadaan et al., 2003), which predicts that the fracture toughness would be higher in a thinner film. The weakest link theory works well for thick films and when inclusion density is high. For polycrystalline silicon tin films of high purity, the geometry effect associated with cleavage front transmission is dominant, which must be taken into consideration in design of microelectromechanical systems, integrated circuits, etc.; otherwise the system reliability would be over-estimated.

Fig. 3 is a micrograph showing a cleavage crack bypassing a triple junction of grain boundaries. It can be seen clearly that, even though the overall film thickness is still small, the crack front is sectioned into two parts. It must propagate separately in different grains along misoriented cleavage planes, which is depicted in Fig. 1(c). In a thin film where the grains are not through-thickness, i.e. if the film has multiple grain layers, as a crack advances through grains "A_i" ($i = 1,2,3$) and reaches the array of grain boundaries, the front must enter grains "B_i" independently, so that each section of it can propagate along the most energetically favorable plane. Thus, the front transmission behaviors are somewhat similar with that shown in Fig. 1(a). It is envisioned that, as the cleavage front is forced to be sectioned by multiple grain layers, the barrier effect of multiple BTWs can enhance the overall fracture resistance, which may provide an important guidance for developing high-toughness thin films. For instance, if during the film deposition process, the crystal growth is interrupted for a few times, with the same film thickness the grain structure can be broken down into a number of layers, which may offer a higher cleavage resistance than a thin film where most of grains are columnar or equiaxed.

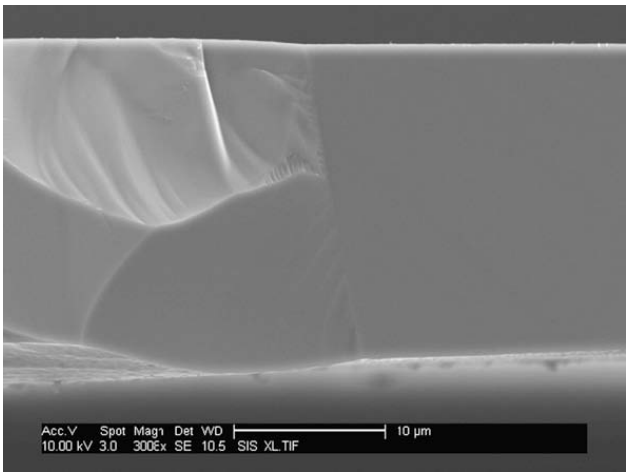

Fig. 3. SEM microscopy of cleavage cracking across a few grain boundaries. The crack propagates from the right to the left.

3. Resistance to cleavage cracking of thin films of multiple grain layers

In order to analyze the details of cleavage resistance of multiple grain layers in a thin film, we consider a quasi-two-dimensional cracking process across a regular array of grain boundaries, as depicted in Fig. 4. The film thickness is t. Along the thickness direction, the grains form a few layers. The grain size, i.e. the layer thickness, is d. Initially, a cleavage front rests along the boundary array ("ab"). The grains behind the boundary array ("A_i"; $i = 1,2\ldots$) are exposed to the precrack surface, and the grains ahead of the boundary array ("B_i") are at the crack tip. The total

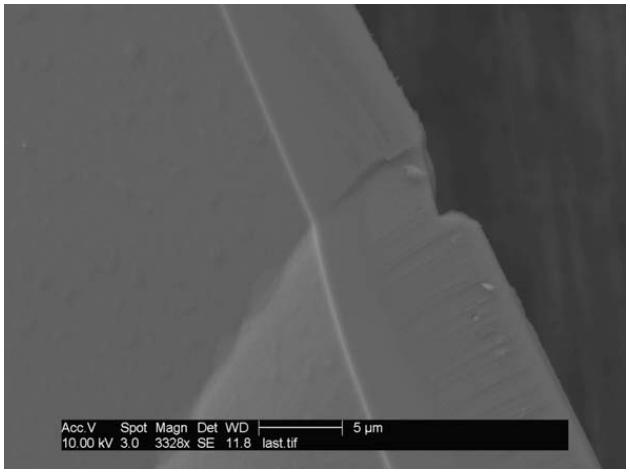

Fig. 2. SEM microscopy of cleavage cracking across a through-thickness grain boundary. The crack propagates from the top to the bottom.

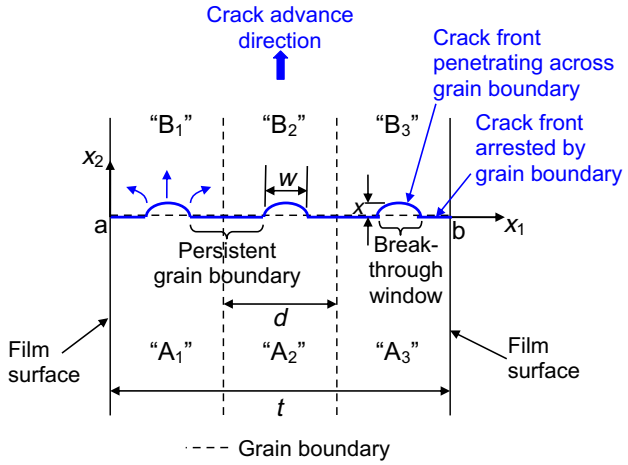

Fig. 4. The top view of the break-through process of a cleavage crack across multiple grain layers.

number of grain layers is N; that is, $t = d{\cdot}N$. Since the film thickness is relatively small, we assume that the free-surface effect on the crack front behavior is uniform along the thickness direction, x_1 (Takashima and Higo, 2005; Janssen and Pujada, 2007).

With the increasing of external loading, the crack growth driving forces rises, and the cleavage front tends to advance into grains "B_i" along axis x_2. The front breaks through the boundary array in a number of break-through windows. Each grain boundary contains one and only one BTW. Inside a BTW, the front penetrate across the boundary stably. The penetration depth is denoted by Δx. In between adjacent BTWs, the front is arrested by PGBA. The relationship between the penetration depth and the BTW width, w, can be described by a power-law function (Qiao, 2003):

$$\frac{w}{d} = \alpha\left(\frac{\Delta x}{d}\right)^{\beta} \tag{1}$$

where α and β are two dimensionless material parameters. If $\alpha = 1$ and $\beta = 2$, the penetrating front section would be a part of circle. Experimental observations show that the actual front sections are much flatter. As a first-order approximation, parameters β can be taken as 1.7.

As the front penetrates deeper into the grains ahead of the boundary array, the BTWs become wider. Since the crack front is no longer straight, the distribution of local crack growth driving force, $G(x_1)$, is non-uniform. At the protruding front sections in BTW, the stress level is lower than that at the concave sections at PGBA, due to the "shielding effect" of the latter. When Δx is relatively small, the local stress intensity factor can be estimated by using a variational method developed by Rice (1985)

$$K(x_1) = K^*(x_2) + \frac{1}{2\pi}\int_X \frac{K^*(\varsigma, x_2)\cdot[x_2(\varsigma) - x_2]}{(\varsigma - x_1)^2}\mathrm{d}\varsigma \tag{2}$$

where x_2 indicates the distance from the crack front to the boundary array, K^* is the reference stress intensity factor for a straight crack front, and "X" indicates the domain occupied by the crack front. Since the front sections arrested at PGBA do not contribute to the variation in local stress intensity factor, Eq. (2) can be rewritten as

$$K(x_1) = K^*(x_2) + \frac{1}{2\pi}\int_{\widehat{X}} \frac{K^*(\varsigma, x_2)\cdot[(\varsigma - x_{1i})/\alpha d]^{1/\beta} d}{(\varsigma - x_1)^2}\mathrm{d}\varsigma \tag{3}$$

where $\widehat{X}$ indicates the crack front sections that penetrate across the boundary array, and x_{1i} is the center of the i-th BTW. Hence, along a PGBA, the average stress intensity factor can be calculated as

$$\bar{K} = K_0 + \frac{K_0 d^{1-1/\beta}}{\pi\alpha^{1/\beta}(d-w)N}\int_{\bar{X}}\int_{\widehat{X}} \frac{(\varsigma - x_{1i})^{1/\beta}}{(\varsigma - x_1)^2}\mathrm{d}\varsigma\mathrm{d}x_1 \tag{4}$$

where $\bar{X}$ indicates the crack front sections arrested by PGBA, w is the BTW width, and K_0 is the reference stress intensity factor if the protruding crack front sections did not exist. As d is replaced by t/N, the above equation becomes

$$\tilde{K} = 1 + \frac{N^{1/\beta}}{\pi\alpha^{1/\beta}(t - Nw)t^{(1-\beta)/\beta}}\int_{\bar{X}}\int_{\widehat{X}} \frac{(\varsigma - x_{1i})^{1/\beta}}{(\varsigma - x_1)^2}\mathrm{d}\varsigma\mathrm{d}x_1 \tag{5}$$

where $\tilde{K} = \bar{K}/K_0$. Thus, the effective crack growth driving force can be assessed as

$$G_{\mathrm{eff}} = \frac{(1-\nu^2)K_0^2}{E}\tilde{K}2 \tag{6}$$

where E and ν are the modulus of elasticity and the Poison's ration, respectively.

Similarly, based on Eq. (2), the local stress intensity factor at the verge of propagating front can be obtained as

$$K^{(i)} = K^*(x_2) - \frac{1}{2\pi}\left[\int_{\bar{X}} \frac{K^*(\varsigma, x_2)\cdot\left\{\Delta x - [(\varsigma - x_{1i})/\alpha d]^{1/\beta} d\right\}}{(\varsigma - x_{1i})^2}\mathrm{d}\varsigma + \int_{\bar{X}} \frac{K^*(\varsigma, x_2)\cdot\Delta x}{(\varsigma - x_{1i})^2}\mathrm{d}\varsigma\right] \tag{7}$$

where $K^{(i)}$ is the local stress intensity factor at the crest of the crack front section in the i-th BTW, and $\Delta x = d{\cdot}(w/\alpha d)^{1/\beta}$ is the penetration depth. Since Δx is usually at the level of 0.1 μm, much smaller than the crack length (e.g. the in-plane grain size, which is typically a few μm to a few mm), for a first-order approximation the variation in K^* can be ignored; that is, $K^* \approx K_0$. Consequently, Eq. (7) is rewritten as

$$\frac{K^{(i)}}{K_0} = 1 - \frac{d}{2\pi}\left[\int_{\widehat{X}} \frac{(w/\alpha d)^{1/\beta} - [(\varsigma - x_{1i})/\alpha d]^{1/\beta}}{(\varsigma - x_{1i})^2}\mathrm{d}\varsigma + \int_{\bar{X}} \frac{(w/\alpha d)^{1/\beta}}{(\varsigma - x_{1i})^2}\mathrm{d}\varsigma\right] \tag{8}$$

According to Eq. (8), the average stress intensity factor at the middle points of protruding front sections in BTWs is

$$\frac{\bar{K}^*}{K_0} = 1 - \frac{d}{2\pi N}\sum_{i=1}^{N}\left[\int_{\widehat{X}} \frac{(w/\alpha d)^{1/\beta} - [(\varsigma - x_{1i})/\alpha d]^{1/\beta}}{(\varsigma - x_{1i})^2}\mathrm{d}\varsigma + \int_{\bar{X}} \frac{(w/\alpha d)^{1/\beta}}{(\varsigma - x_{1i})^2}\mathrm{d}\varsigma\right] \tag{9}$$

In Eq. (9), Δx and w should be regarded as the average values of penetration depth and BTW width along the crack front, respectively.

Since the crack front sections in BTWs propagate stably in the grains ahead of the boundary array, the effective local crack growth driving force, $\bar{G}^*$, must be equal to the local fracture resistance, i.e.

$$\bar{G}^* = \bar{G}_{\mathrm{B}} = \frac{1}{N}\sum_{i=1}^{N} G_{\mathrm{B}}^{(i)} \tag{10}$$

where $G_{\mathrm{B}}^{(i)}$ is the resistance to cleavage cracking of the crystallographic plane of grain "B_i". For a brittle material, the stress and strain fields are dominated by the linear elastic deformation. Hence,

$$\bar{K}^* = \sqrt{\frac{E\bar{G}^*}{1-\nu^2}} \tag{11}$$

Combination of Eqs. (9)–(11) gives

$$K_0 = \sqrt{\frac{E\bar{G}_B}{1-\nu^2}} \Bigg/ \left\{ 1 - \frac{d}{2\pi N} \sum_{i=1}^{N} \left[\int_{\bar{x}} \frac{(w/\alpha d)^{1/\beta} - [(\varsigma - x_{1i})/\alpha d]^{1/\beta}}{(\varsigma - x_{1i})^2} d\varsigma + \int_{\bar{x}} \frac{(w/\alpha d)^{1/\beta}}{(\varsigma - x_{1i})^2} d\varsigma \right] \right\} \tag{12}$$

Substitution of Eqs. (5) and (12) into Eq. (6) leads to

$$\frac{G_{\text{eff}}}{\bar{G}_B} = \frac{\left(1 + \frac{N^{1/\beta}}{\pi\alpha^{1/\beta}(t-Nw)t^{(1-\beta)/\beta}} \int_{\bar{X}} \int_{\bar{X}} \frac{(\varsigma - x_{1i})^{1/\beta}}{(\varsigma - x_1)^2} d\varsigma dx_1\right)^2}{1 - \frac{t}{2\pi N^2} \sum_{i=1}^{N} \left[\int_{\bar{x}} \frac{(wN/\alpha t)^{1/\beta} - [(\varsigma - x_{1i})N/\alpha t]^{1/\beta}}{(\varsigma - x_{1i})^2} d\varsigma + \int_{\bar{x}} \frac{(wN/\alpha t)^{1/\beta}}{(\varsigma - x_{1i})^2} d\varsigma \right]} \tag{13}$$

The calculation result of Eq. (13) indicates that G_{eff} increases with w, as it should, since the stress concentration at the arrested crack front sections becomes more pronounced as the BTWs are wider.

As the crack front advances, the effective crack growth driving force must overcome the local fracture resistance, R. A material offers resistance to fracture because work must be done to generate cracks. During the process that the cleavage front penetrates across the boundary array, the work of separation is

$$W = W_B + W_{gb} \tag{14}$$

where W_B is the fracture work associated with cracking on crystallographic planes in grains "B_i", and W_{gb} is the fracture work associated with separation of grain boundary areas in BTWs. They can be calculated as

$$W_B = \sum_{i=1}^{N} G_{Bi} \cdot A_0 = \frac{2N}{\alpha^{1/\beta}} \frac{\beta}{(1+\beta)d^{1/\beta - 1}} \left(\frac{w}{2}\right)^{1+1/\beta} \cdot \bar{G}_B \tag{15}$$

and

$$W_{gb} = \sum_{i=1}^{N} G_{gb} \cdot \frac{w^2}{2} \tan\theta_i = N \cdot \frac{w^2 G_{gb}}{2} \cdot \bar{\Theta} \tag{16}$$

where A_0 is the area of the fracture facet in grain "B_i", i.e. the area exposed by the penetrating crack front section; G_{gb} is the effective work of separation of grain boundary; θ_i is the twist misorientation angle of grain "B_i" with respect to grain "A_i"; and $\bar{\Theta}$ is the average value of $\tan\theta_i$. The effective resistance to BTW expansion can then be obtained as

$$R = \frac{1}{t}\frac{dW}{dw} = \frac{\beta \bar{G}_B}{2 + \beta + 1/\beta} \left(\frac{Nw}{2\alpha t}\right)^{1/\beta} + \frac{N\bar{\Theta} G_{gb} w}{t} \tag{17}$$

Clearly, R increases with w. When the external loading is small, the crack growth driving force, G_{eff}, is smaller than the BTW expansion resistance, R, and therefore the crack front cannot penetrate across the boundary array. With the increasing of applied loading, the stress intensity at crack tip rises. When $G_{\text{eff}} = R$, the crack front reaches an equilibrium condition, and with a small disturbance the front sections would advance in grains "B_i" in BTWs, leading to the increase in w. However, because R increase rapidly with w, after w changes by an infinitesimal increment, G_{eff} becomes smaller than R again, so that the BTW expansion ceases, until the external loading is further increased. That is, under this condition, the crack front behavior is stable.

As w becomes larger, the penetration depth of front sections in BTWs increases. The increase rate of R is

$$\frac{dR}{dw} = \frac{\bar{G}_B}{2 + \beta + 1/\beta} \left(\frac{N}{2\alpha t}\right)^{1/\beta} \frac{1}{w^{1-1/\beta}} + \frac{N\bar{\Theta} G_{gb}}{t}, \tag{18}$$

and the increase rate of G_{eff} is

$$\frac{dG_{\text{eff}}}{dw} = \bar{G}_B f' \tag{19}$$

where f' is the first-order derivative of the right-hand side of Eq. (13) with respect to w. Note that the integration domains, $\bar{x}$ and $\bar{X}$ are also functions of the BTW width. Since β is typically larger than 1 (Qiao, 2003), i.e. the protruding crack front sections are convex, through Eq. (18) it can be seen that while dR/dw is always positive, it decreases with w. The increase rate of G_{eff}, however, rises as w becomes larger. Thus, there exists a critical point at which not only

$$G_{\text{eff}} = R, \tag{20}$$

but also

$$dG_{\text{eff}}/dw = dR/dw. \tag{21}$$

Under this condition, similar to the principle of classic R-curve analysis (Kannien and Popelar, 1985), with a small variation in BTW width, the increase rate of crack growth driving force becomes larger than that of fracture resistance, and the crack front would keep moving forward; that is, the crack propagation is unstable. Thus, Eqs. (13), (17), and (18)–(21) provide a complete set of governing equations that determine the critical condition of final failure of the grain boundary array.

4. Results and discussion

While R and $dR/d\Delta x$ have closed-form solutions, G_{eff} and $dG_{\text{eff}}/d\Delta x$ must be solved numerically. In order to understand the effects of grain structure on cleavage cracking resistance, a model problem is analyzed in detail. The film thickness, t, is set to 5 μm, close to the thicknesses of thin-film samples in which the crack front behaviors are dominated by single break-through points (Qiao and Kong, 2007). Note that since this model is scalable, the value of t does not affect the calculation result of grain boundary fracture resistance. The number of grain layers, N, varies from 1 to 10. When $N = 1$, the problem is reduced to the through-thickness grain boundary case. According to the measurement of directions of river markings, parameter β is taken as 1.7 (Qiao, 2003). The effective fracture resistance of grain "B_i" is assessed as

$$G_{Bi} = \frac{G_{cry}}{\cos\theta_i \cos\psi_i} \tag{22}$$

where $G_{cry} \approx 15\ \text{J/m}^2$ is the fracture resistance of crystallographic plane of silicon (Ohring, 1992), and θ_i and ψ_i are the twist and the tile misorientation angles of grain "B_i" with respect to grain "A_i" ($i = 1, 2 \ldots N$), respectively. For the sake of simplicity, θ_i and ψ_i are set to the middle point of their ranges of variation (either + 22.5° or −22.5°), and thus $\bar{G}_B = 1.17 G_{cry}$ and $\bar{\Theta} = 0.41$. The value of G_{gb} is around $0.8 G_{cry}$. The factor of 0.8 is typical for semiconductors such

as silicon (Gilman, 1960; Hondros and Stuart, 1968; Flewitt and Wild, 2001).

With a given value of N, the grain structure and the break-through mode of cleavage front are pre-determined. Initially, w was set to a small value of $10^{-3}t$. Through Eq. (17), the resistance to BTW expansion, R, can be calculated as a function of α. When the cleavage front penetrates across the boundary array, the break-through windows must expand, and thus Eq. (20) should be satisfied. Combination of Eqs. (13), (17), and (20) leads to

$$\left[\frac{N\bar{\Theta}w}{t}\left(\frac{G_{gb}}{\bar{G}_B}\right)+\frac{\beta}{2+\beta+1/\beta}\left(\frac{Nw}{2\alpha t}\right)^{1/\beta}\right]\cdot g(\alpha) = \left(1+\frac{N^{1/\beta}}{\pi\alpha^{1/\beta}(t-Nw)t^{(1-\beta)/\beta}}\int_{\bar{x}}\int_{\hat{x}}\frac{(\varsigma-x_{1i})^{1/\beta}}{(\varsigma-x_1)^2}\mathrm{d}\varsigma\mathrm{d}x_1\right)^2$$

where

$$g(\alpha)=1-\frac{t}{2\pi N^2}\times\sum_{i=1}^{N}\left[\int_{\hat{x}}\frac{(wN/\alpha t)^{1/\beta}-[(\varsigma-x_{1i})N/\alpha t]^{1/\beta}}{(\varsigma-x_{1i})^2}\mathrm{d}\varsigma+\int_{\bar{x}}\frac{(wN/\alpha t)^{1/\beta}}{(\varsigma-x_{1i})^2}\mathrm{d}\varsigma\right] \quad (23)$$

solving which gives α, and thus the penetration depth can be calculated. By using Eqs. (18) and (19), $\mathrm{d}G_{eff}/\mathrm{d}w$ and $\mathrm{d}R/\mathrm{d}w$ are obtained and compared with each other. If the former is smaller, the crack front penetration is stable. The value of w is increased by $10^{-3}t$ and the above procedure is repeated. Eventually, since $\mathrm{d}G_{eff}/\mathrm{d}w$ increases with w and $\mathrm{d}R/\mathrm{d}w$ decreases with w, at a critical BTW width the latter would be equal to or smaller than the former. Under this condition, the BTW develops unstably, at which the value of G_{eff} is the peak resistance that the grain boundary array can offer. The numerical results are shown in Fig. 5, where $G_{cr}^{(N)}$ indicates the critical fracture resistance of the grain boundary array of N grain layers.

When N increases, since the crack front penetrates the grain boundary array at a larger number of locations, the break-through mode is somewhat similar with that in a large bicrystal, except that the distance between adjacent BTWs are smaller and the cleavage facets ahead of the boundary array are no longer parallel to each other. As a result, the fracture resistance of the grain boundary array, R, tends to increase with N, as shown by Eq. (17). With the same BTW width, the external loading must be increased to a higher level so that the effective crack growth driving force can overcome the fracture resistance. Consequently, compared with thin films of the same thickness but fewer grain layers, the boundary toughness is larger. As shown in Fig. 5, when the number of grain layers, N, changes from 1 to 4–5, $G_{cr}^{(N)}$ increases by 50–60%. This size effect is distinct from the weakest link theory, which should be negligible when the length scale is small and the content of impurity is low. The dependence of $G_{cr}^{(N)}$ on N, or the grain size, d, discussed above is associated with the confinement effect of lateral grain boundaries on cleavage front transmission.

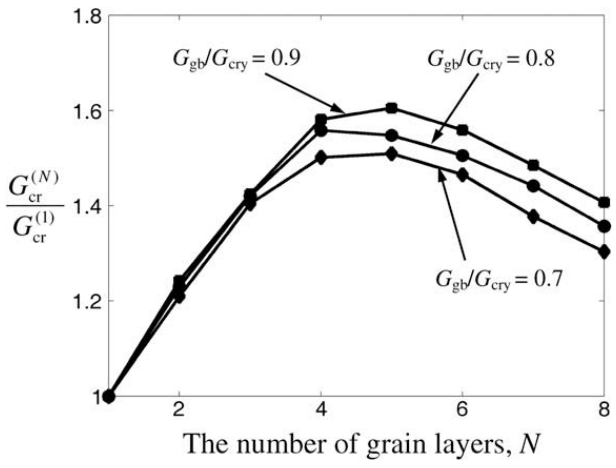

Fig. 5. The fracture toughness as a function of the number of grain layers. The tilt and twist misorientation angles are set to ±22.5°.

When N further increases from 4–5 to 8, however, the fracture resistance of the boundary array is reduced, primarily because that $\mathrm{d}G_{eff}/\mathrm{d}w$ also increases with N. On the one hand, as more break-through windows are formed along the crack front, the shielding effect of PGBA is more significant. To reach $\bar{G}_B$ at the verge of propagating front, as w varies the change in reference stress intensity factor, K_0, must be larger. On the other hand, even with the same K_0, since the penetrating front sections contribute less to the overall crack growth driving force, the local energy release rate at PGBA, i.e. the driving force of BTW expansion, rises, and thus it is more sensitive to the increase in BTW width. Hence, with the same R–w relationship, the critical condition of unstable front advance would be reached at a smaller BTW width, so that G_{cr} tends to decrease.

The two competing mechanisms result in an optimum grain layer number, $N_{opt}\approx 4$–5, at which $G_{cr}^{(N)}$ is maximized. When N is relatively small, the effect of fracture resistance is dominant, and $\mathrm{d}G_{cr}^{(N)}/\mathrm{d}N$ is positive. When $N > N_{opt}$, the influence of variation rate of effective crack growth driving force is more pronounced, and $\mathrm{d}G_{cr}^{(N)}/\mathrm{d}N$ is negative. This result provides an important mechanism for toughening brittle thin-film materials. If during film deposition, the grain growth along the film thickness direction can be interrupted by a few times, e.g. by changing deposition rate, using appropriate dopants, adjusting substrate temperature, and/or stopping and resuming deposition process, a controlled number of grain layers can be formed. If $N = N_{opt}$, without changing the overall film thickness, the fracture properties can be considerably improved, satisfying the increasingly high functional requirements on system reliability and structural integrity.

The fracture resistance of the boundary array is also dependent on the separation work of grain boundary, as it should be. As demonstrated in Fig. 5, as G_{gb} becomes larger, $G_{cr}^{(N)}$ rises. This effect is relative less evident when $N < 3$, since the break-through mode of the cleavage front should be quite stable if there are only a small number of break-through points. When $N \geqslant 4$, $G_{cr}^{(N)}$ increases significantly with G_{gb}. When G_{gb}/G_{cry} increases from 0.7 for 0.9, $G_{cr}^{(N)}$ rises by 10–15%, indicating that the effect of grain boundary separation is amplified by the multiple crack front sections. With the increasing of G_{gb}, the optimum value of N also increases slightly from 4 to 5, which may be attributed to that G_{gb} comes in by affecting the effective resistance to

BTW expansion. Since for most brittle semiconductors the value of G_{gb}/G_{cry} is close to 0.8, G_{gb} should be regarded as a secondary factor compared with the grain size effect.

Another important factor that affects the overall fracture resistance of the grain boundary array is the crystallographic misorientation, which, in this study, is captured by the average fracture resistance of grains "B_i", $\bar{G}_B$ and the average value of tan θ_i, $\bar{\Theta}$. The former is determined by both twist and tilt misorientation angles, and the latter is related to only twist misorientation. As shown in Fig. 6, as the average twist angle, $\bar{\theta}$ or the average tilt angle, $\bar{\psi}$ become larger, the critical fracture resistance increases, which is in agreement with the observations of fracture in large bicrystals (Qiao and Argon, 2003a,b). As the misorientation angles increase, first, the area of fracture surface is larger, so that the work of separation of the grains ahead of the boundary array increases. Second, more grain boundary area needs to be separated apart so that the fracture surfaces across the boundary array can be connected. Fig. 6 indicates that the influence of the twist angle is more significant compared with the tilt angle. When $\bar{\theta}$ changes from 5° to 30°, $G_{cr}^{(N)}$ varies by nearly 20%. When $\bar{\psi}$ changes in the same range, the variation in $G_{cr}^{(N)}$ is only less than 10%. The effects of $\bar{\theta}$ and $\bar{\psi}$ are dependent on the number of grain layers. When N is changed from 4 to 8, the sensitivity of $G_{cr}^{(N)}$ to $\bar{\theta}$ and $\bar{\psi}$ is reduced, which is compatible with the results shown in Fig. 5 that, if $N > N_{opt}$, the overall fracture resistance decreases as the grains are finer.

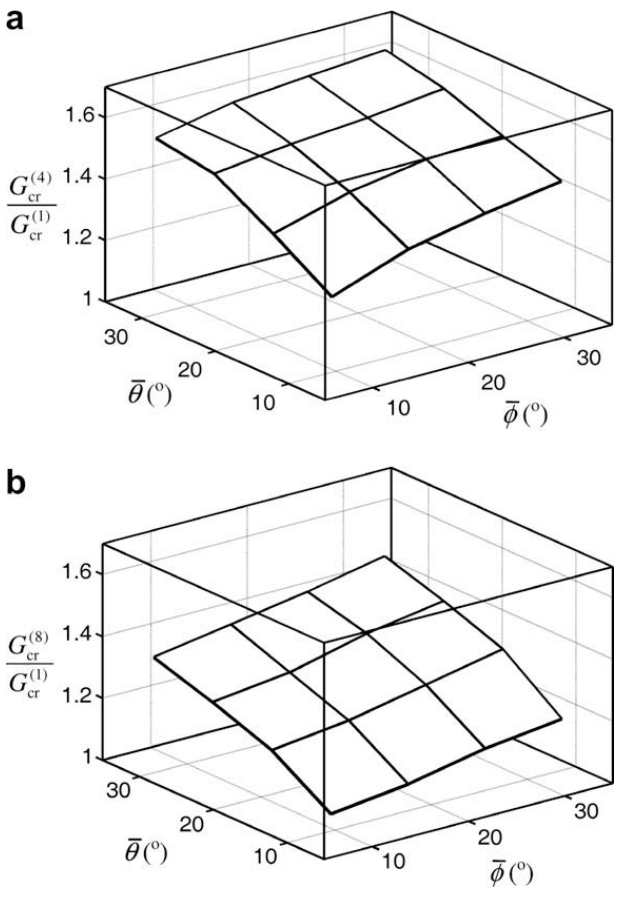

Fig. 6. The fracture toughness as a function of the crystallographic misorientation angles: (a) $N = 4$ and (b) $N = 8$.

5. Concluding remarks

A theoretical analysis is performed on the resistance of a regular grain boundary array to cleavage cracking in a free-standing brittle thin film. If the grains are through-thickness, due to the confinement effect of film surfaces, there would be only a single break-through window along the cleavage front, and thus when the film thickness is reduced the grain boundary toughness is lower than in a large bicrystal. In the grain size is smaller than the film thickness, i.e. if the film contains multiple grain layers, the cleavage front must be geometrically necessarily broken down into a number of sections, so that the cleavage cracking can take place on misoriented cleavage planes in the grains ahead of the boundary array. As a result, the cleavage front transmission process is somewhat similar with that in a large bicrystal, and the overall fracture resistance is higher. Since the sensitivity of effective crack growth driving force to the grain structure also increases with the number of grain layers, if the grain size is too small, further decreasing it would have a detrimental effect. According to the numerical result, the optimum number of grain layers is 4–5, depending on the work of separation of grain boundary. The boundary toughness is also related to the crystallographic misorientation angles across the boundary array. The twist misorientation angle has a more pronounced effect than the tilt angle. These results provide a promising way for improving toughness of thin film materials.

Acknowledgement

This work was supported by The Department of Energy under Grant No. DE-FG02-05ER46195.

References

Bagdahn, J., Sharpe, W.N., Jadaan, O., 2003. Fracture strength of polysilicon at stress concentrations. J. MEMS 12, 302–312.
Bakker, A., 1992. Three-dimensional constraint effects on stress intensity distribution in plate geometries with through-thickness cracks. Fatigue Fract. Eng. Mater. Struct. 15, 1051–1059.
Boyce, B.L., Grazier, J.M., Buchheit, T.E., Shaw, M.J., 2007. Strength distribution in polycrystalline silicon MEME. J. MEME 16, 179–190.
Flewitt, P.E.J., Wild, R.K., 2001. Grain Boundaries – Their Microstructures and Chemistry. Wiley, NY.
Gell, M., Smith, E., 1967. The propagation of cracks through grain boundaries in polycrystalline 3% silicon iron. Acta Metall. 15, 253–258.
Gilman, J.J., 1960. Direct measurements of the surface energies of crystals. J. Appl. Phys. 31, 2208–2218.
Greek, S., Ericson, F., Johansson, S., Schweitz, J., 1997. In situ tensile strength measurement and Weibull analysis of thick film and thin film micromachined polysilicon structures. Thin Solid Films 292, 247.
Greek, S., Ericson, F., Hohansson, S., Furtsch, M., Rump, A., 1999. Mechanical characterization of thick polysilicon films: Young's modulus and fracture strength evaluated with microstructures. J. Micromech. Microeng. 9, 245.
Hahn, G.T., Averback, B.L., Owen, W.S., Cohen, M., 1959. Initiation of cleavage microcracks in polycrystalline iron and steel. In: Averback, B.L., Felbeck, D.K., Hahn, G.T., Thomas, D.A. (Eds.), Fracture. MIT Press, Cambridge, MA, pp. 91–116.
Haque, M.A., Saif, M.T.A., 2003. A review of MEMS-based microscale and nanoscale tensile and bending testing. Exp. Mech. 43, 248–255.

Hondros, E.D., Stuart, E.H., 1968. Interfacial energies of textured silicon iron in the presence of oxygen. Philos. Mag. 17, 711–727.
Jackson, M.J., 2003. Microfabrication and Nanofabrication. CRC Press, Boca Raton, FL.
Jadaan, O.M., Nemeth, N.N., Bagdahn, J., Sharpe, W.N., 2003. Probabilistic Weibull behavior and mechanical properties of MEMS brittle materials. J. Mater. Sci. 38, 4087–4113.
Janssen, M., 2004. Fracture Mechanics. Taylor & Francis, NY.
Janssen, G.C.A.M., Pujada, B.R., 2007. Elastic deformation of silicon (001) wafers due to thin film stresses. Appl. Phys. Lett. 91, 121913.
Jensen, B.D., de Boer, M.P., Masters, N.D., Bitsie, F., LaVan, D.A., 2001. Interferometry of actuated microcantilevers to determine material properties and test structure nonidealities in MEMS. J. MEMS 10, 336.
Kahn, H., Heuer, A.H., Ballarini, R., 2001. On-chip testing of mechanical properties of MEMS devices. MRS Bull. 26, 300.
Kannien, M.F., Popelar, C.H., 1985. Advanced Fracture Mechanics. Oxford University Press, NY.
Kong, X., Qiao, Y., 2005. Crack trapping effect of persistent grain boundary islands. Fatigue Fract. Eng. Mater. Struct. 28, 753–758.
Lau, J.H., Wong, C.P., Prince, J.L., 1998. Electronic Packaging – Design Materials Process and Reliability. McGraw-Hill, NY.
Madou, M.J., 2002. Fundamentals of Microfabrication. CRC Press, Boca Raton, FL.
McClintock, F.A., 1997. A three dimensional model for polycrystalline cleavage and problems in cleavage after extended plastic flow or cracking. In: Chan, K.S. (Ed.), Cleavage Fracture – George R. Irwin Symposium Proceedings. TMS, Warrendale, PA, p. 81.
Muhlstein, C.L., 2005. Characterization of structural films using microelectromechanical resonators. Fatigue Fract. Eng. Mater. Struct. 28, 711–721.
Ohring, M., 1992. The Materials Science of Thin Films. Academic Press.
Qiao, Y., 2003. Modeling of resistance curve of high-angle grain boundary in Fe–3wt%Si alloy. Mater. Sci. Eng. A 361, 350–357.
Qiao, Y., Argon, A.S., 2003a. Cleavage crack growth resistance of grain boundaries in polycrystalline Fe–2wt%Si alloy: experimentals and modeling. Mech. Mater. 35, 129–154.
Qiao, Y., Argon, A.S., 2003b. Cleavage crack growth resistance of high angle grain boundaries in Fe–3wt%Si alloy. Mech. Mater. 35, 313–331.
Qiao, Y., 2005a. The role of recalcitrant grain boundaries in cleavage cracking in polycrystals. J. Mater. Sci. 40, 4819–4825.
Qiao, Y., 2005b. Irregular-mode cracking in Fe–3wt%Si alloy. J. Mater. Sci. Technol. 21, 338–342.
Qiao, Y., Chen, J., 2008. Resistance of through-thickness grain boundaries to cleavage cracking in silicon thin films. Scripta Mater. 59, 251–254.
Qiao, Y., Kong, X., 2007. On size effect of cleavage cracking in polycrystalline thin films. Mech. Mater. 39, 746–752.
Rice, J.R., 1985. First-order variation in elastic fields due to variation in location of a planar crack front. J. Appl. Mech. 52, 571–579.
Schweitz, J., Ericson, F., 1999. Evaluation of mechanical materials properties by means of surface micromachined structures. Sensors Actuators A74, 126.
Sharpe, W.N., Yuan, B., Edwards, R.L., 1997. A new technique for measuring the mechanical properties of thin films. J. Micromech. Microeng. 6, 193.
Srikar, V.T., Spearing, S.M., 2003. A critical review of microscale mechanical testing methods used in the design of microelectromechanical systems. Exp. Mech. 43, 238–247.
Takashima, K., Higo, Y., 2005. Fatigue and fracture of a Ni–P amorphous alloy thin film on the micrometer scale. Fatigue Fract. Eng. Mater. Struct. 28, 703–710.
Wu, Z.X., 2006. On the through-thickness crack with a curve front in center-cracked tension specimens. Eng. Fract. Mech. 73, 2600–2613.